ADVANCED ENERGY MATERIALS
www.advenergymat.de

An Emerging Solid-State Electrolyte Reactor to Drive the Future of Electrochemical Synthesis

*Weisong Li, Yanjie Zhai, Qing Xia, and Xiao Zhang**

Electrochemical reactors, powered by renewable electricity, have garnered widespread attention for chemical synthesis due to their low energy consumption and pollution-free features. However, the inherent design flaw of traditional electrochemical reactors has persistently hindered the advancement of electrochemical synthesis, as they result in low product concentrations, low purity, and continuous production issues. As a novel electrochemical reactor, the porous solid-state electrolyte (PSE) reactor is elaborately designed to overcome the limitation by enabling the direct and continuous synthesis of pure products, possessing a modular and scalable structure with high efficiency, safety, and long stability. In this work, first, the distinctive design of the PSE reactor, highlighting its structural features, core components, and variable configurations, is introduced. Furthermore, the configuration-relevant applications in electrosynthesis, such as formic acid, acetic acid, and hydrogen peroxide (H_2O_2) production, are summarized. Integrated applications are also discussed, along with potential domains for improvements and optimization. Finally, the future developmental directions of the PSE devices are thoroughly explored. By addressing its unique design attributes, showcasing its capabilities, and envisioning prospective refinements and diverse applications, the aim is to boost the progression of this transformative technology toward widespread commercialization and industrial adoption, thereby revolutionizing sustainable electrochemical synthesis.

1. Introductions

The synthesis and production of chemicals are indispensable prerequisites for human survival and development. Given the pressing energy crisis and severe environmental pollution issues, there is an urgent demand for the development of chemical synthesis methods that can contribute to energy conservation and emissions reduction. Electrochemical production of valuable chemicals has garnered significant interest in the research community, owing to its unique environmental and energy-related advantages over traditional thermochemical synthesis methods.[1–3] While the mainstream point has been predominantly focused on designing and synthesizing electrocatalysts to enhance product purity, selectivity, and yield,[4,5] the development and fabrication of efficient electrochemical devices are equally crucial for improving conversion rates and stability. Notably, conventional electrochemical devices often have inherent design flaws that result in the target products being mixed with the electrolyte or the reactants, leading to purity issues and subsequent separation/purification costs.[6–11] These issues are frequently overlooked but inevitably present in electrochemical synthesis and contribute to overwhelming extra energy costs. To address this, a novel porous solid-state electrolyte (PSE) reactor has been developed with a meticulously engineered additional buffer compartment enclosed by anion and cation membranes.[12] This design facilitates the direct synthesis of pure products, thereby eliminating the purity problems.

Different from conventional proton exchange membrane (PEM) and anion exchange membrane (AEM) reactors, a PSE reactor features a three-chambered design, where the middle compartment decouples product formation, providing a buffer space for ion recombination of target products. Current literature on the utilization of the PSE reactor remains sparse, primarily limited to the synthesis of simple products, such as formic acid,[13] acetic acid,[14] and H_2O_2.[12] Furthermore, only limited review papers focus on the structures and applications of PSE reactors.[15–18] Evidently, the existing research lacks a comprehensive and holistic understanding of the PSE reactors in terms of the structures, key components, and variable configurations. In this Perspective, we emphasize the capabilities of the PSE reactor

W. Li, Y. Zhai, Q. Xia, X. Zhang
Department of Mechanical Engineering
The Hong Kong Polytechnic University
Hung Hom, Kowloon, Hong Kong SAR 999077, China
E-mail: xiao1.zhang@polyu.edu.hk
W. Li, X. Zhang
Research Institute for Advanced Manufacturing
The Hong Kong Polytechnic University
Hung Hom, Kowloon, Hong Kong SAR 999077, China
X. Zhang
Research Institute for Smart Energy
The Hong Kong Polytechnic University
Hung Hom, Kowloon, Hong Kong SAR 999077, China

The ORCID identification number(s) for the author(s) of this article can be found under https://doi.org/10.1002/aenm.202403841

DOI: 10.1002/aenm.202403841

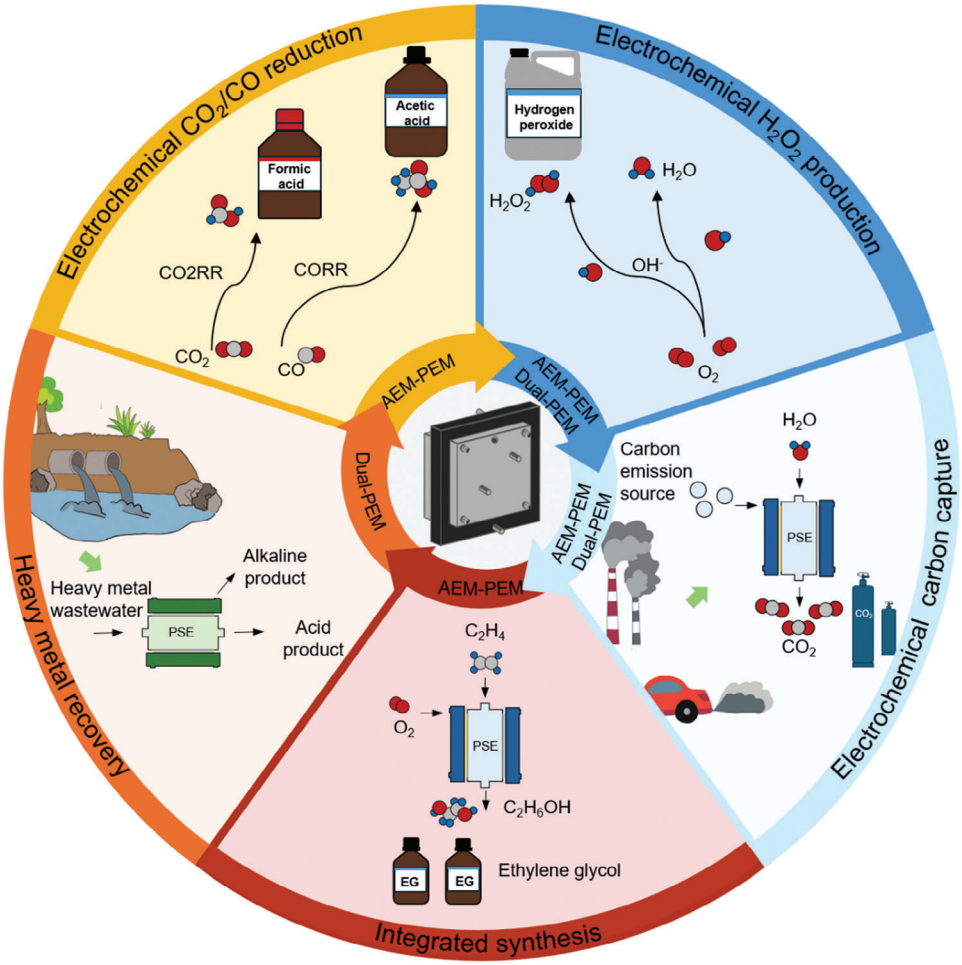

Figure 1. The summary of the PSE reactor configurations and their corresponding applications, including liquid fuels provided by CO_2RR and CORR, H_2O_2 generated by oxygen reduction reaction (ORR), electrochemical CO_2 capture, ethylene glycol (EG) production, and future utilization on heavy metal recovery.

in electrochemical carbon dioxide reduction reaction (CO_2RR), carbon monoxide reduction reaction (CORR), H_2O_2 synthesis, CO_2 capture, and related integrated applications, as depicted in **Figure** 1. Additionally, we propose feasible optimization strategies and outline future application paths to propel the PSE reactor technology toward widespread commercial adoption, advancing electrochemical synthesis into a new era of sustainability and scalability.

2. Structure and Configuration

Conventional electrochemical reactors such as H-type cells (**Figure** 2a), flow cells (Figure 2b), and membrane electrode assembly (MEA) cells (Figure 2c) face inherent challenges due to the undesirable mixing of reactants or electrolytes with products, which impedes the ability to obtain high-purity and high-concentration products.[7,8] An H-type cell is the most fundamental electrochemical device, which consists of two connected chambers and a membrane that separates the cathode and anode liquids. The electrosynthesis reaction usually occurs at the cathode, and its products are mixed with the imprinted electrolyte. As the reaction proceeds, the reaction rate and yield will gradually decrease, which makes a noncontinuous production. The upgraded version of the H-type cell is the flow cell, which reduces the distance between the cathode and the anode region. The cathode electrolyte and the reactants flow and update continuously to realize continuous production, in which a part of the ohmic loss is reduced. The MEA reactor further reduces the distance between the cathode and the anode region and adopts membrane hot-pressing electrode technology to achieve long-term stable electrosynthesis. However, the problem is that the liquid products are typically mixed with reactants or electrolytes, and thus further separation and purification processes are required, resulting in extra energy consumption. These energy costs make the low-energy and pollution-free green synthesis advantages of electrochemical synthesis no longer competitive. In contrast, the PSE reactor features a sandwich-like design and a double-membrane system, which is equipped with a middle chamber and ion exchange membranes to decouple ion formation and recombination. This design boosts the direct synthesis of high-purity products without the need for additional purification and separation processes, as depicted in Figure 2d.

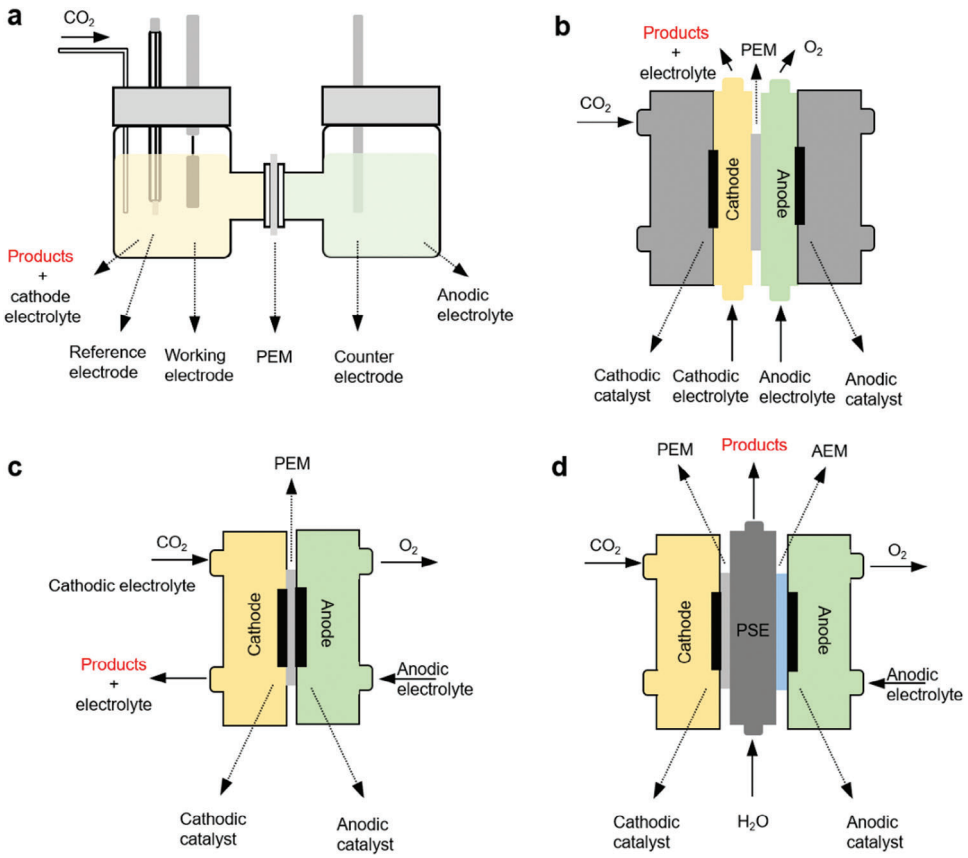

Figure 2. The schematic diagrams illustrate the various electrolytic devices, including a) H-cell, b) flow cell, c) MEA cell, and d) PSE reactor, all in the context of electrochemical CO_2 reduction. The yellow regions represent the cathode chambers, while the green areas denote the anode chambers. The gray connecting components are designated as PEMs, and the yellow component represents an AEM. The deep gray chamber in the PSE reactor corresponds to the middle PSE chamber. In the conventional cell architectures, the products become intermixed with the electrolytes or reactants while the PSE reactor design incorporates two membranes and a buffer chamber that facilitate the separation and formation of target products in the middle chamber.

Specifically, the typical PSE device can be described as a symmetric, sandwich-like structure, as illustrated in **Figure** 3a. It comprises the following key components: cathodic and anodic catalysts with corresponding diffusion layer (DL), PEM and AEM, and a middle plate filled with solid-state electrolytes in the central window. The auxiliary accessories include the polar plates equipped with flow channels, gaskets, screws, and nuts. The sizes of the catalyst sheets, diffusion layers, membranes, and gasket windows can be flexibly adjusted for different application scenarios. This symmetric, multilayered design of the PSE reactor allows for efficient electrochemical processes and optimized mass/energy transport and regulation within the system. The customizable core components offer flexibility for diverse applications, allowing for the tailoring of current density, productivity, and yield.

In the components of PSE devices, the solid-state electrolytes serve as the key elements, playing a crucial role in ion recombination and the separation of pure products. The solid-state electrolytes can be classified into anionic and cationic polymer conductors, which are functionalized with different conductive organic functional groups[19,20] and inorganic components.[21] To maximize the ion transport efficiency and reduce the energy loss in an electrochemical system, it is important to screen and optimize the composition of PSE. In a previous study by Millar et al., the sulfonate-group functionalized styrene-divinylbenzene dimers were synthesized,[22] and exhibited good performance to conduct protons.[23] For electrochemical applications, the modified proton transfer polymer ionic conductors exhibit good processability, flexibility, and stability in lithium-ion batteries.[24] In 2019, Wang's group successfully employed the functionalized proton conductors (styrene-divinylbenzene dipolymers) as the PSE to realize pure H_2O_2 production[12] and formic acid production.[13] Typically, the functionalized sulfonic acid groups ($-SO_3H$) enable effective proton (H^+) combination and transfer. The commercially available products of the polymers are in the shape of microbeads, for example, Dowex 50 WX8 (H-form). In addition to the proton conductivity, the compact but porous PSE ensures the sufficient fluidity of the gas or liquid streams, so that the products can flow out of the middle plate smoothly and therefore achieve the separation and purification of the products. The PSE is filled into the slotted middle plate and closely wrapped by membranes on the left and right sides. To avoid short circuits and corrosive issues in the middle chamber,[25] black polyoxymethylene (POM) is normally used to fabricate the middle plate.

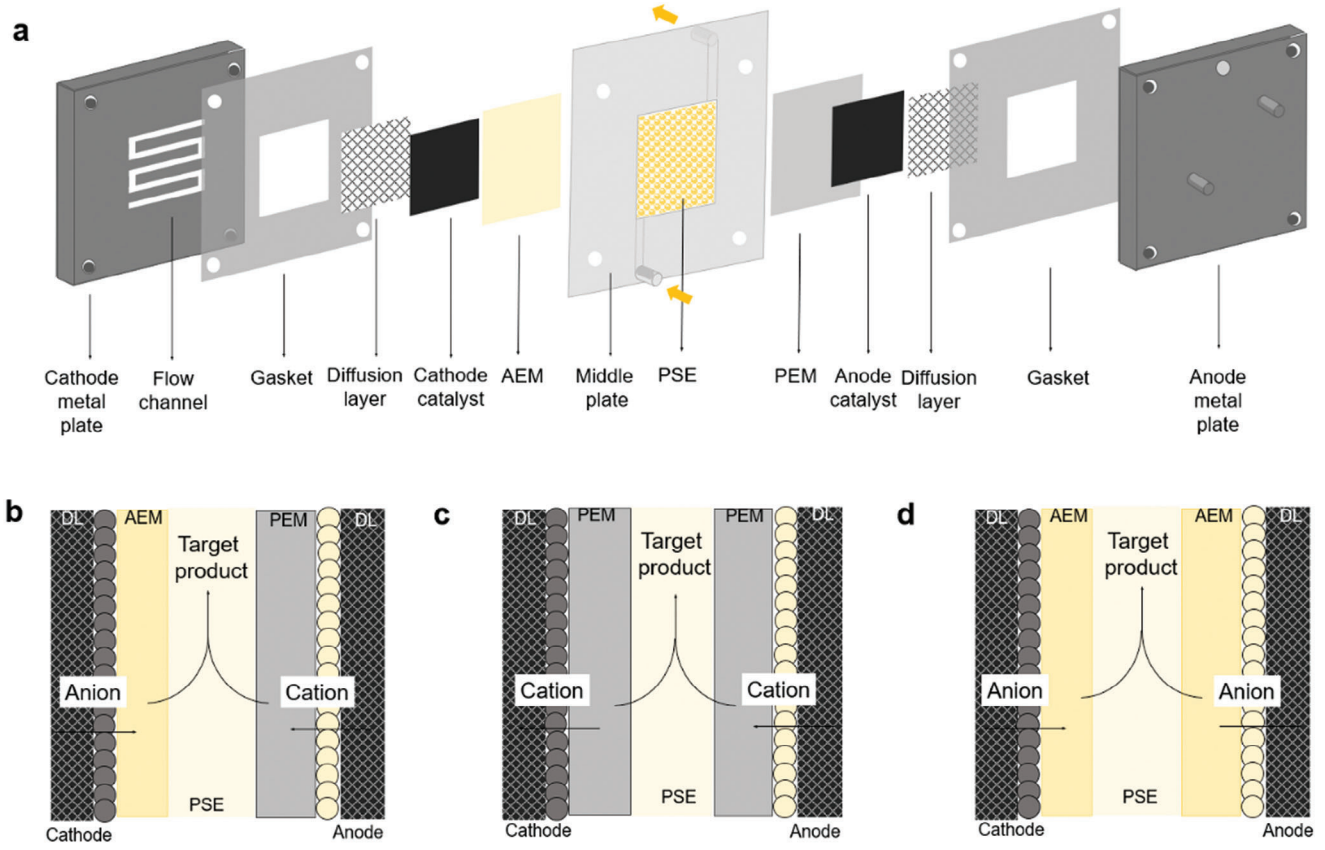

Figure 3. a) The structural components of a typical PSE reactor. The main components are as follows: polar metal plates, flow fields, gaskets, DL, AEM and PEM, catalyst sheets, and a middle chamber. All the electrode plates and the middle plate are designed with gas/liquid inlets and outlets. Additionally, the metal plates, middle plates, and the gaskets are equipped with screw holes and electrode clamp holes. This carefully engineered, multilayered configuration allows for efficient electrochemical reactions and optimized mass/energy transfer and control within the system. The strategic placement of inlets/outlets and the inclusion of clamping mechanisms enable a robust and modular reactor design with adaptability. The different cell configurations involve b) AEM-PEM type, c) dual-PEM type, and d) dual-AEM type.

According to Zhu's experiments and analysis, the thickness of the middle plate makes a considerable contribution to the overall resistance and therefore leads to the corresponding shifts in energy consumption.[26] In addition, the middle plate is also designed with inlet and outlet channels to ensure the product can be smoothly taken away by the flowing medium.

Beyond the core components, the diverse configurations of the PSE reactor also enable their broad range of applications. The PEM-AEM type, as depicted in Figure 3b, is the most common configuration, used for applications such as CO_2RR to formic acid,[13] CORR to acetic acid,[14] and ORR to H_2O_2.[12] This simple but effective design leverages the selective separation of target ions through the strategic placement of AEM-PEM type, enabling the desired ionic recombination within the PSE reactor to directly yield the pure target products. The dual-PEM configuration, on the other hand, enables for more specialized applications (Figure 3c). Willauer et al. designed an electrolytic cation exchange module to liberate CO_2 wherein hydrogen evolution reaction (HER) occurs in the cathode chamber, producing hydrogen and NaOH. Meanwhile, protons generated from the OER at the anode react with the seawater in the middle chamber to liberate the dissolved CO_2.[27,28] This strategy conveys the idea that customized chemical reactions can be performed by taking advantage of the directional movement of ions in the PSE middle chamber. The dual-PEM system benefits from the exceptional stability and performance of Nafion (commercial PEM) membrane, which outperforms the AEM-PEM configuration in long-term operational viability. In Figure 3d, a novel PSE configuration, dual-AEM type, is proposed, which features a fully symmetric configuration, incorporating double AEMs at both anode and cathode chamber. Such symmetry is supposed to ensure uniform anion transport and optimize reaction performance. Additionally, by utilizing ion-selective AEMs, this structure holds the potential to promote customized reactions in the middle chamber. This configuration theoretically enables two types of applications. First, it facilitates the exchange and separation of anions in the central chamber, wherein, under the influence of an electric field, anions at the cathode migrate through the AEM into the central chamber, while anions intended for separation migrate toward the anode, thereby achieving ion separation and recombination. Second, it could fully exploits the anions in the cathode region, allowing them to traverse the entire system to the anode region for the desired oxidation reactions, thus enabling the electrosynthesis of products in the anode chamber. However, the utilization of this configuration has not yet been realized due to the inherent stability issues of AEMs and their weak resistance

to strong acidic/alkaline environments.[29–31] Future research directions warrant a more in-depth investigation into this promising approach. This configuration holds significant promise, as it could enable the tailored synthesis of pure target products through the selective management of anionic species within the reactor. The diverse configuration of PSE reactors each with its own strengths and specialized applications, underscore the versatility and customizability of this technology. By carefully selecting the appropriate membrane architecture and operational parameters, researchers and engineers can harness the full potential of the PSE reactor to address a wide range of electrochemical synthesis challenges and unlock new avenues for sustainable, high-purity chemical production.

3. Emerging Applications of PSE Reactors

3.1. AEM-PEM Type Configuration for Carbon Reduction and Oxygen Reduction

3.1.1. Mechanism Introduction

The PSE reactor technology holds a pivotal position in the domain of carbon reduction and oxygen reduction. The current major applications of PSE reactors are focused on CO_2 reduction to formic acid, CO reduction to acetic acid, and oxygen reduction to H_2O_2. These applications have effectively leveraged the AEM-PEM configuration, as depicted in Figure 3b. The key principle underlying these applications is the selective separation and recombination of the target anionic and cationic species generated at the respective electrodes. Specifically, the anionic species produced at the cathode during the reductive half-reaction are selectively transported through AEM, while the protons generated at the anode during the oxidative half-reaction are selectively transported through the proton PEM. This spatial decoupling and strategic ionic transport mechanism facilitates the direct formation of the desired pure target products within the middle compartment of the PSE reactor.

The micro-surface where electrochemical reactions take place is referred to as the triple phase boundary (TPB).[32] This concept is widely accepted and extensively analyzed in the research field of fuel cells, and it is also highly applicable to the study of electrolyzers. As shown in **Figure 4a**, the star-marked regions represent the TPBs within the PSE reactor. At these critical interfaces, the electrocatalysts constitute the solid phase, the CO_2, CO, or O_2 are in the gas phase, and the water molecules are in the liquid phase. The successful operation of the electrochemical reactions relies on the coordinated mass transfer from the gas phase, the ion conduction facilitated by the membranes, and the electron and ion conduction enabled by the catalyst materials. In this context, the catalyst plays a pivotal role in determining the selectivity toward the target product, in this case, formic acid, acetic acid, or H_2O_2. Therefore, the effective utilization of the catalyst is crucial for the selective production of liquid fuels in the PSE reactor system.

3.1.2. Carbon Reduction in PSE Devices

Despite the inherent challenge of requiring relatively high overpotentials and purity issues for electrochemical CO_2RR, promising advancements have been made in producing formic acid using solid electrolyte reactors. Several research groups have successfully demonstrated the electrosynthesis of formic acid through PSE reactors, highlighting the potential of this reactor utilization.[13,33–37] Extensive studies on various catalyst systems indicate that the selectivity and stability of formic acid production are closely linked to the specific characteristics of the catalysts employed. **Table 1** provides a comprehensive summary of the catalysts investigated and their corresponding performance parameters. These findings underscore the critical role of catalyst design and optimization in enhancing the efficiency and feasibility of the CO_2 reduction process within PSE reactor frameworks. By fine-tuning catalyst performance, researchers have effectively addressed the inherent energy barriers associated with CO_2 reduction, paving the way for the development of more efficient and sustainable pathways for formic acid production.

Among the various electrocatalysts for CO_2 reduction to formic acid, Bismuth (Bi) has emerged as one of the most promising catalysts for carbon dioxide reduction reactions (CO_2RR),[38,39] demonstrating remarkable catalytic activity and selectivity in formic acid production. Compared to other referable catalysts such as tin (Sn) and lead (Pb), Bi-based catalysts exhibit a stronger affinity for the key precursor intermediate, *OCO, while also enhancing binding capabilities.[40] Consequently, researchers have explored various strategies to optimize the performance of Bi-based catalysts for formic acid synthesis. Xia et al. proposed a simple and versatile 2D design for Bi particles, achieving a Faradaic efficiency (FE) of 93.1% while producing pure formic acid at concentrations approaching 30% (Figures 4b,c).[13] Zhu et al. synthesized defect-rich Bi_2S_3 nanowires (NWs) and demonstrated their durability for formic acid production over 120 h.[34] Yang et al. reported the use of Bi_2O_3 for continuous production of HCOOH over 1000 h, albeit with a selectivity of ≈82%.[37]

Since significant progress has been made in developing Bi-based electrocatalysts, their synthesis approaches often involve time-consuming and complex processes. Notably, the electrochemical durability of these reported Bi-based catalysts may fall short of industrial-scale application requirements. To address these challenges, current research is focused on creating a more scalable and stable alternative catalyst, thereby enhancing the feasibility of formic acid production via carbon dioxide reduction. For instance, Yang et al. examined conventional Sn catalysts, achieving a FE of 94% for formic acid at a current density of 140 mA cm^{-2}, though this was achieved at a higher voltage of 3.5 V.[36] Additionally, Zheng et al. fabricated a lead-copper (Pb-Cu) alloy catalyst and demonstrated a high FE of 96% for formic acid, with a durability of 180 h at a current density of 100 mA cm^{-2} in a PSE reactor.[35] While advancements in tin-based and lead-based catalysts have partially enhanced the durability and selectivity of formic acid production driven by CO_2RR, it is essential to prioritize the continuous improvement of catalysts and the development of cost-effective, scalable synthesis strategies in research agendas. These efforts are crucial for further enhancing the feasibility and industrial potential of electrochemical CO_2 reduction for formic acid production. Current research focuses on optimizing catalyst performance, refining synthesis methods, and addressing challenges related to long-term stability. Such initiatives are vital for fully realizing the

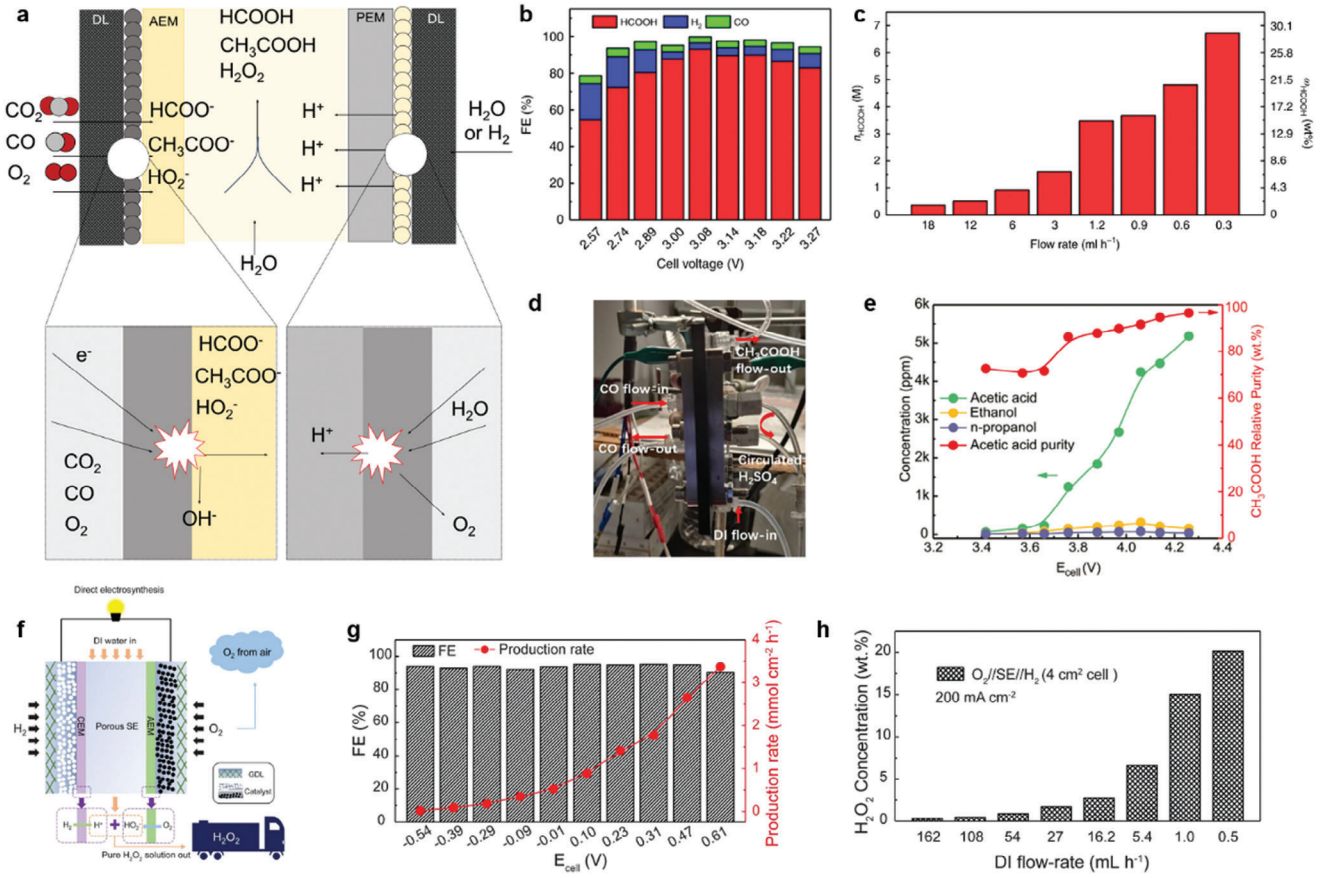

Figure 4. a) The schematic diagram illustrates the electrochemical carbon reduction and oxygen reduction processes within a PSE reactor, highlighting the critical role of the TPB. In this system, the DL and the catalyst layer (CL) are depicted. The spark mark symbolizes the position of the TPB, where the gas phase (CO_2/CO/O_2), liquid phase (water), and solid phase (catalyst) intersect. The electrochemical performance of CO_2RR to formic acid production on b) FE and c) concentration.[13] Copyright 2019, Springer Nature. d) The system design for acetic acid production in the PSE reactor features a CO inlet and outlet on the left side, a circulated anode electrolyte within the right metal plate, and a water inlet with the CH_3COOH outlet deployed on the middle plate.[14] e) Purity and concentration of acetic acid produced by CORR.[14] Copyright 2021, PNAS. f) The schematic illustration of H_2O_2 production by ORR and HOR coupling.[12] g) The FE and production rates of H_2O_2 under different cell voltages.[12] h) H_2O_2 concentration under different DI water flow rates.[12] Copyright 2019, AAAS.

potential of electrochemical CO_2 reduction as a viable and sustainable pathway for producing valuable formic acid.

Electrochemical CO_2RR using PSE reactors has not only made good progress in formic acid synthesis, but also contributed to initial progress for the synthesis of other C_{2+} products, including ethanol, n-propanol, and acetic acid, as demonstrated by Wang's research group.[13] However, the detection of only 1 mM of acetic acid at a high applied voltage of 3.45 V indicates a limited selectivity of existing electrocatalysts for the direct reduction of CO_2 to acetic acid. It has been established that the direct reduction of CO_2 to acetic acid typically requires the formation of CO intermediates as a crucial step.[41] Therefore, a key strategy to enhance

Table 1. The materials and performance parameters on formic acid production by PSE reactors in the publications.

Cathode catalysts	Top FE_{HCOOH} [%] (@ j_{HCOOH} (mA cm^{-2}))	Durability [h] (@ j_{HCOOH} (mA cm^{-2}))	C_{HCOOH} [M] (@ j_{HCOOH} (mA cm^{-2}))	Refs.
2D-Bi	93.1 (32.1)	100 (30)	0.112 (30)	[13]
nBuLi-Bi	≈97 (440)	100 (30)	≈0.62 (30)	[33]
Bi_2S_3 nanowires	>80 (50)	120 (30)	N/A	[34]
Pb_1Cu	≈94 (375)	180 (100)	0.16 (100)	[35]
Sn	≈94 (140)	500 (100)	≈0.02 (100)	[36]
Bi_2O_3	≈93 (200)	1000 (200)	≈1.3 (100)	[37]

Table 2. The materials and performance parameters on acetic acid production by PSE reactors in the publications.

Cathode catalysts	Top $FE_{CH3COOH}$ [%] (@ $j_{CH3COOH}$ (mA cm^{-2}))	Durability [h] (@ $j_{CH3COOH}$ (mA cm^{-2}))	$C_{CH3COOH}$ [mM] (@ $j_{CH3COOH}$ (mA cm^{-2}))	Refs.
Cu_2O nanotubes	43	10 (@200 mA)	≈50	[14]
Gb-Cu	56.5	120 (@200 mA)	90	[43]
Cu-CN	46	140 (@250 mA)	≈76	[42]

the performance of PSE reactors for acetic acid production is the design and development of electrocatalysts capable of effectively stabilizing and activating these CO intermediates. By engineering catalysts with improved CO adsorption and activation characteristics, both the selectivity and efficiency of the direct conversion of CO_2 to acetic acid can be significantly enhanced. Due to the limitations of directly CO_2RR to acetic acid using PSE reactors, some researchers have explored alternative methods that utilize CO as a reactant for acetic acid production through PSE devices.[14,42,43] As illustrated in Figure 4a, CO molecules are reduced at the cathode to form acetate ions (CH_3COO^-). Subsequently, protons generated from water (H_2O) combine with the acetate ions in the intermediate PSE layer to produce the final acetic acid product. Pure CH_3COOH can then be extracted by passing water through the central PSE chamber (Figure 4d). Zhu et al. synthesized Cu_2O nanotubes, achieving a purity of up to 98% for CH_3COOH at a concentration of 86 mM (Figure 4e).[14] Zheng et al. developed a grain boundary-rich Cu(Gb-Cu) catalyst, resulting in an acetic acid concentration of 516.1 mM with a durability of 140 h.[42] (**Table 2**) However, it is important to note that the efficiency, purity, stability, and energy consumption for producing acetic acid remain significantly lower compared to formic acid. This highlights the needv for further research and development to enhance the performance of CO_2 reduction catalysts and reactor systems, specifically targeting the production of acetic acid.

3.1.3. Oxygen Reduction in PSE Devices

PSE reactors also play a crucial and unique role in the electrochemical production of H_2O_2. To address the challenges associated with product mixtures in liquid electrolytes, Xia et al. proposed the utilization of the solid electrolytes in the middle chamber to obtain pure H_2O_2.[12] As illustrated in Figure 4f, the two-electron ORR ($2e^-$-ORR) ($O_2 + 2e^- + H_2O \rightarrow HO_2^- + OH^-$) occurs in the cathode chamber. The produced HO_2^- can then migrate into the anion exchange membrane (AEM) and reach the middle chamber. In the opposite chamber, the hydrogen oxidation reaction (HOR) is involved to generate protons ($H_2 \rightarrow 2e^- + 2H^+$). Alternatively, the oxygen evolution reaction (OER) can also be employed to provide a proton supply. The produced H^+ can then cross the PEM and combine with HO_2^- to produce H_2O_2. By flowing a water stream, the pure H_2O_2 product can be collected and stored. Xia's work has achieved a selectivity of 90% under a current density of 200 mA cm^{-2}(Figure 4g) and a concentration of 20% under a DI water flow rate of 0.5 mL h^{-1}(Figure 4h).[12] To further enhance the activity and selectivity, another study was conducted by employing a carbon black catalyst doped with boron (B-C) in the same PSE cell structure, achieving a FE of 95% under a current density of 400 mA cm^{-2}.[44] In contrast, Zhang et al. investigated the cation effect on H2O2 production using the commerically available BP2000 catalyst, achieving a FE of 90% while maintaining stability for over 500 h.[45] Meanwhile. Rawah et al. developed a nitrogen-doped carbon (N-C) material and adjusted its hydrophobic properties, resulting in a FE greater than 90% at a current density of 389 mA cm^{-2}.[46] (**Table 3**). Despite thses significant advancements, improving the stability of H_2O_2 production in PSE devices under high current density remains a considerable challenge.

Table 3. The materials and performance parameters on H_2O_2 production by PSE reactors in the publications.

Cathode catalysts	Top FE_{H2O2} [%] (@ j_{H2O2} (mA cm^{-2}))	Durability [h] (@ j_{H2O2} (mA cm^{-2}))	C_{H2O2} [mM] (@ j_{H2O2} (mA cm^{-2}))	Refs.
XC-72	>90 (200)	100 (120)	0.30 (120)	[12]
B-C	95 (400)	200 (30)	0.03 (30)	[44]
BP2000	≈90 (50)	500 (50)	0.15 (50)	[45]
N-C	>90 (389)	50 (389)	220 (389)	[46]

3.1.4. Further Utilization of AEM-PEM Type PSE Devices

Electrochemical CO_2 Capture: In conventional CO_2RR, several researchers have observed the issue of CO_2 crossover, which occurs under elevated current densities and leads to an overestimation of the catalytic performance.[47,48] During the CO_2RR process, hydroxide (OH^-) ions are produced, either as accompanying the target reduction products or directly from the competitive HER ($2H_2O + 2e^- \rightarrow 2OH^- + H_2$). These hydroxide ions can then absorb CO_2 molecules to form carbonate (CO_3^{2-}) ions ($CO_2 + 2OH^- \rightarrow CO_3^{2-} + H_2O$). Driven by the external electric field, the CO_3^{2-} ions can permeate across the AEM and combine with protons generated from the anode. This leads to the liberation of CO_2 molecules ($CO_3^{2-} + 2H^+ \rightarrow CO_2 + H_2O$), which then mix with the O_2 molecules and flow out of the electrochemical cell. To address the issue of CO_2 loss, Kim et al. proposed a CO_2 recovery strategy by leveraging a PSE reactor.[49] The employment of a middle PSE chamber capitalizes on the inherent process of CO_2 crossover and release in the MEA cell. Owing to the use of a PEM on the anode side, the recovered CO_2 will not mix with O_2 but can be flushed out to be recirculated back to the cathode gas inlet. This innovative strategy provides a novel perspective for the utilization of PSE reactors, expanding their

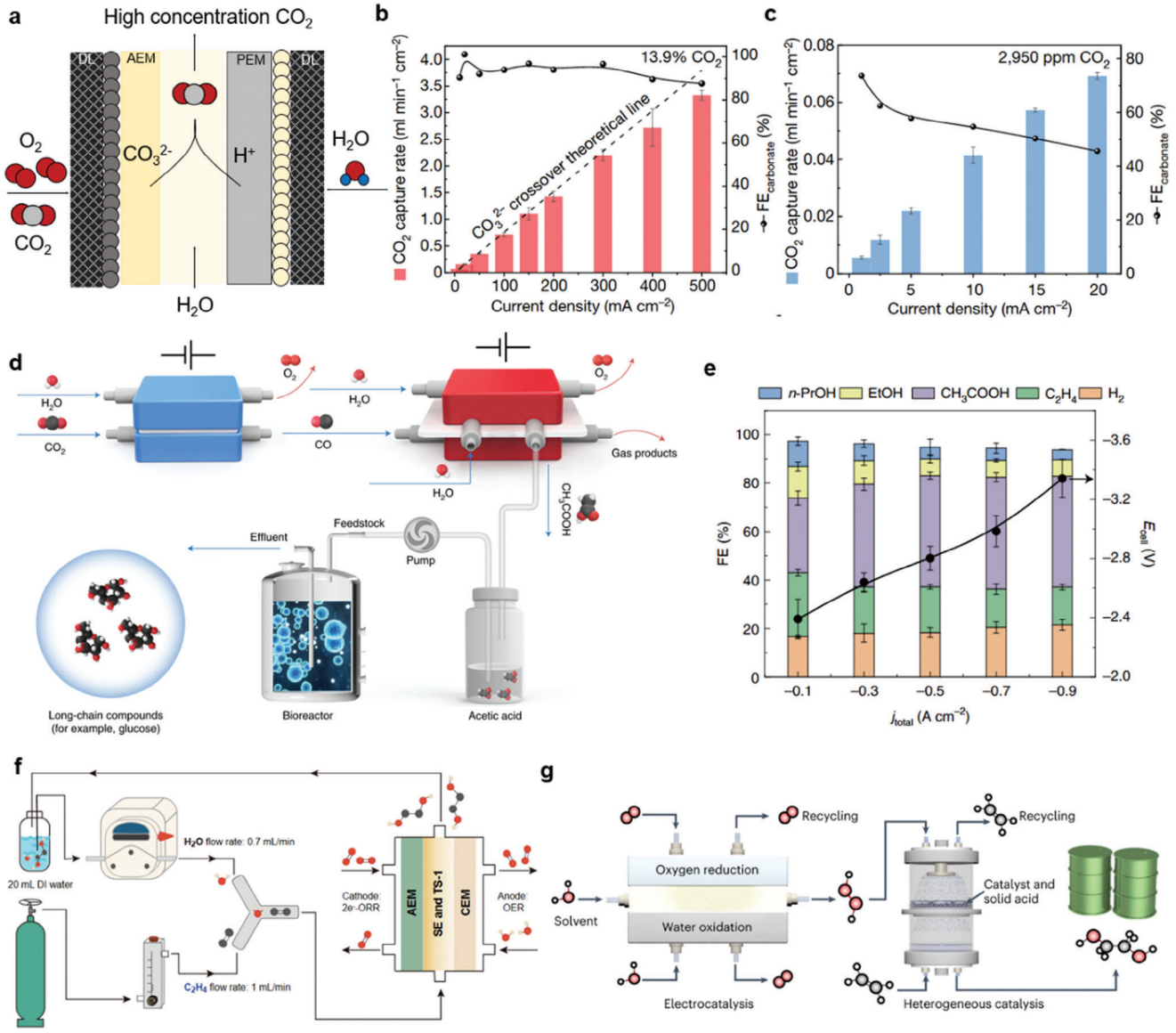

Figure 5. a) AEM-PEM strategy for CO_2 capture from the gas mixture. The electrochemical performance of the CO_2 capture system under b) 13.9% CO_2 and c) 2950 ppm CO_2.[26] Copyright 2023, Springer Nature. d) The schematic diagram of the CO_2RR/CORR upgrading system, wherein CO_2 undergoes reduction to CO, and further reduction to CH_3COOH, then it is pumped into a bioreactor to feed yeast and produce long-chain products.[42] e) The production of pure acetic acid by the PSE reactor, where the blue, light yellow, purple, green, and orange colors stand for normal propanol (n-PrOH), ethanol (EtOH), acetic acid (CH_3COOH), ethylene (C_2H_4) and hydrogen (H_2), respectively.[42] Copyright 2022, Springer Nature. f) The integrated system design for EG production. The EG formation happens in the middle chamber with the in-site produced H_2O_2.[51] Copyright 2023, Elsevier. g) The cascade system design for EG production. A thermocatalytic reactor is combined with the electrochemical H_2O_2 production reactor.[50] Copyright 2021, Springer Nature.

application directions beyond merely the production of pure liquid products. By enabling the recovery and recycling of the CO_2 that would otherwise be lost, this approach demonstrates the versatility and potential of PSE reactors in enhancing the efficiency and sustainability of electrochemical CO_2 conversion processes. Zhu et al. further expanded the application of proton-selective exchange (PSE) reactors to CO_2 gas capture and concentration by exploiting the carbon crossover phenomenon.[26] As illustrated in **Figure** 5a, the cathode is supplied with a mixture of O_2 and CO_2, catalyzed by platinum-supported carbon (Pt/C). The four-electron ORR (4e$^-$-ORR) ($O_2 + 4e^- + 2H_2O \rightarrow 4OH^-$) can occur at the cathode to produce OH^- ions, which then capture the CO_2 molecules. As shown in Figures 5b,c, the ratio of the inlet gas mixture was changed from 13.9% to 2950 ppm to simulate the real CO_2 concentrations in flue gas and air. The results demonstrate that the PSE reactor can achieve nearly 99% FE under an industrially relevant current density of 300 mA cm^{-2}. For ppm-level CO_2 capture, the FE is ≈75% under 20 mA cm^{-2}. This work lays a solid foundation for the application of PSE reactors in CO_2 capture and separation, showcasing their versatility and potential

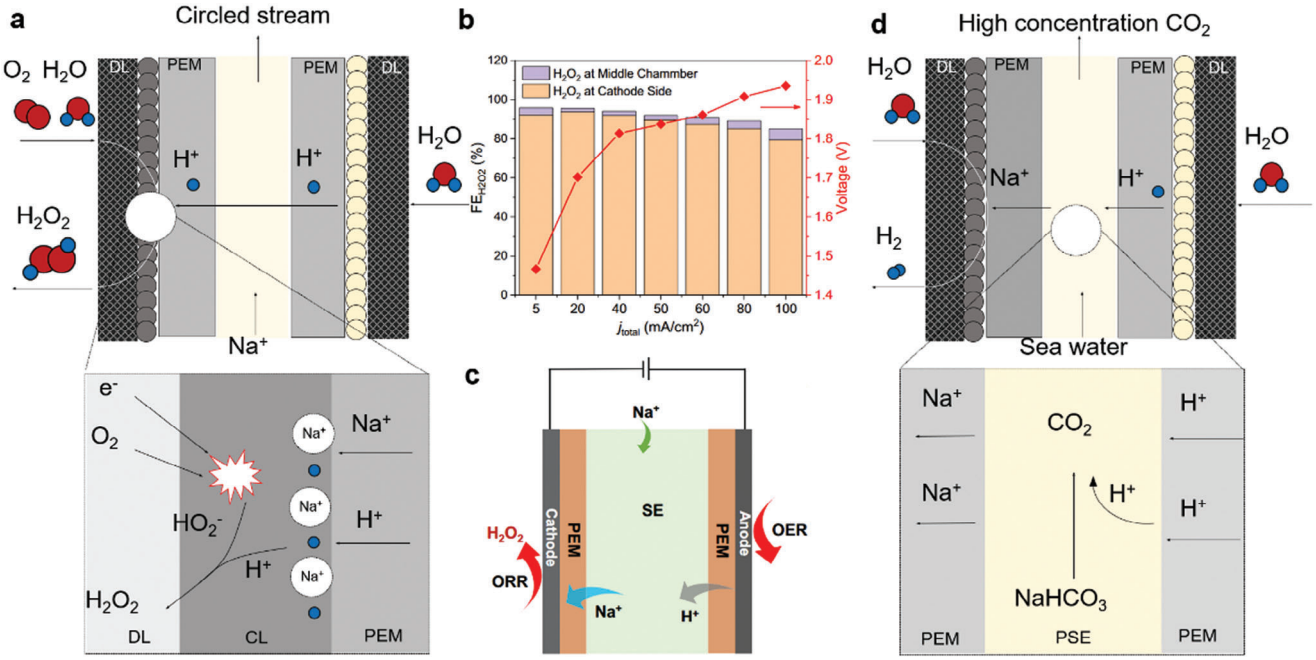

Figure 6. a) The applications of dual-PEM configuration in PSE reactors. b) The FE of H_2O_2 under different current densities and c) cell configuration.[45] Copyright 2022, Springer Nature. d) Electrochemical CO_2 capture from seawater.

in addressing the challenges of low-concentration CO_2 capture and enabling efficient CO_2 utilization.

CO_2RR/CORR Coupling Systems: PSE reactors have demonstrated remarkable performance in the synthesis of mono- and di-organic acids. Several researchers have begun to design coupled systems to realize the application of PSE reactors in small molecule synthesis.[43] The strategy of using PSE reactors for CO_2RR and CORR to generate pure products has flexible utilization potential due to the modular structure, facile assembly methods, and mild operation conditions. Zheng et al. employed a coupled system to convert the production of CH_3COOH by CO_2RR and CORR into the synthesis of long-chain compounds, assisted by a bioreactor as shown in Figure 5d.[45] First, CO_2 is electro-reduced to CO by a nickel-nitrogen-carbon (Ni–N–C) single-atom catalyst with nearly 100% FE in a flow cell. The separated CO product is then pumped into the PSE reactor and catalyzed by a GB–Cu catalyst to generate pure CH_3COOH with a FE of 46% and a purity of ≈97% (Figure 5e). The pure acetic acid product is subsequently fed into a bioreactor for yeast fermentation, which generates glucose and free fatty acids. This coupling strategy can be easily scaled to achieve a variety of long-chain products from CO_2 through specific microbial conversion approaches, thus opening new possibilities for electrically driven manufacturing.

H_2O_2 Coupling Systems: H_2O_2, as an active oxidant, can be utilized to synthesize small molecules in the PSE device. For instance, Fan et al. reported a tandem system for H_2O_2 production, which was then combined with ethylene for the synthesis of EG (Figure 5f).[50] This cascade system can achieve over 95% FE for H_2O_2 production and an electron efficiency for EG production larger than 60% under a current density of 10 mA cm^{-2}. Alternatively, Zhang et al. designed an integrated system to directly produce EG in a PSE reactor (Figure 5g).[51] The middle PSE chamber is mixed with molecular sieve catalysts (TS-1) and proton-exchange copolymers. In this setup, the in-situ generated H_2O_2 can directly undergo an addition reaction with the ethylene flowing into the middle chamber, synthesizing EG under the catalysis of TS-1. The production rate is detected to be over 500 μmol h^{-1}, and the maximum FE of EG can reach 63% after 3 h of reaction. Importantly, by utilizing the in-situ generated species, the proposed integrated strategy goes beyond conventional electrochemical EG production and opens a wide range of applications. It effectively eliminates the requirement for energy-intensive purification processes, offering adaptability and versatility in harnessing the potential of electrochemically driven manufacturing using PSE reactors.

3.2. Dual-PEM Type Configuration in PSE Reactor Utilization

The previously proposed strategy for H_2O_2 production exhibited relatively low durability (<200 h) due to stability issues with the catalyst and the anion membranes. Zhang et al. proposed a novel PSE cell configuration with dual-PEM configuration.[45] As depicted in **Figure 6a**, this configuration involves substituting the AEM with a PEM. This allows the protons generated by OER to directly migrate from the anode to the cathode. However, the direct proton flow creates a strongly acidic environment surrounding the catalyst surface, leading to further reduction of H_2O_2 into H_2O.[52] To mitigate the local acidity, alkali metal ions such as sodium (Na^+) and potassium (K^+) are pumped into the middle PSE layer. Driven by the electric field, these alkali metal ions can also traverse the PEM to the cathode side, exerting a repulsive effect on the protons and forming a local basic microenvironment.

This design aims to ensure that the combination of HO_2^- and H^+ occurs in the cathode chamber, allowing the pure H_2O_2 product to be flushed out by a humidified oxygen stream. This strategy to produce H_2O_2 in the cathode chamber achieved a FE of 90% under 50 mA cm^{-2} (Figure 6b).

In addition to the utilization in H_2O_2 production, several researchers have considered the dual-PEM strategy for CO_2 capture from seawater.[27,28] Under natural conditions, CO_2 from the atmosphere dissolves into seawater and exists in the form of bicarbonate (HCO_3^-) and CO_3^{2-} ions. The inherent composition of seawater enables its potential use as a carrier to release the captured CO_2. Willauer et al. designed an electrolytic cation exchange module to liberate the CO_2 (Figure 6d).[27,28] In this system, the HER occurs in the cathode chamber, producing hydrogen and sodium hydroxide (NaOH). Concurrently, protons generated from the OER at the anode react with the seawater in the middle chamber to liberate the dissolved CO_2. This strategy exemplifies how customized chemical reactions can be performed by taking advantage of the directional movement of ions in the PSE middle chamber. This allows for the generation of pure products not only from the middle layer but also in the electrode chambers, providing a novel perspective on the structural applications of PSE reactors. Interestingly, Chen et al. employed the dual-PEM to achieve the nitrate conversion to ammonia by a similar cation regulation strategy.[53] The dual-PEM system can effectively leverage the cationic modulation within the middle chamber to fully harness the cathode reduction reaction. This technology holds significant potential for future investigation in nitrate/nitrite reduction and CO_2/CO reduction of multi-carbon products.

4. Future Applications of PSE Devices

Given the considerable applications of PSE devices demonstrated in CO_2 capture, basic-cathode (CO_2RR, CORR, ORR or HER), and acidic-anode reactions (OER or HOR), it is foreseeable that gas separation and acid-base regulated ion separation could have the potential to be achieved by tuning the cell configurations, catalyst materials, electrode reactions, and middle layer reactions. For gas separation, it has been proven that CO_2 can be effectively captured and separated from gas mixtures with air-level concentrations from Zhu' work.[26] Motivated by the basic environment provided by the cathode reactions, other acidic gases could also be absorbed and converted into anions by the PSE reactors. The migrated anions could then combine with the protons from the anode side to form pollution-free inorganic salts. Meanwhile, the acidic gases can be separated into fresh air, enabling a promising and renewable strategy for air purification (**Figure** 7a). This approach will not only address the challenge of gas separation but also offer a sustainable pathway for producing valuable acid products while simultaneously purifying the air. The versatility and adaptability of PSE reactors in these applications will demonstrate their significant potential in addressing environmental and industrial challenges.

Another potential application of PSE reactors can be observed in the realm of heavy metal ion recovery. As reported by Willauer et al., a double-PEM acidic electrolytic modular system can be employed, whereby the feedstock can be directly pumped into the middle chamber to facilitate the desired reactions, and an alkaline solution can be generated in the cathode chamber.[27,28] This strategic approach indicates that multiple ionic reactions can be harnessed within the PSE chamber and the cathode chamber to achieve the sought-after separation effect. As illustrated in Figure 7b, heavy metal salts can be directly introduced into the middle chamber, driven by the electric field force. The heavy metal cations can then migrate across the PEM and combine with the hydroxide ions produced by the cathodic reactions, culminating in the formation of a heavy metal alkaline solution. Concurrently, the remaining anions from the heavy metal salts can react with the protons moving from the anode, thereby generating inorganic acid. This integrated system has the potential to effectively mitigate the prevailing issues of high energy consumption and elevated pollution levels associated with conventional heavy metal recycling processes. By leveraging the unique capabilities of PSE reactors, the selective recovery and separation of heavy metal ions can be accomplished more sustainably and efficiently.

5. Future Improvements of PSE Devices

The practical deployment of PSE devices faces a series of challenges, including high energy consumption, exorbitant material costs, low product yield, failure to achieve industrially relevant current density, and poor system stability. As such, the following measures can be adopted to further optimize the utilization of energy and materials, as well as enhance the overall performance of the reactor (Figure 7c).

First, the architectural design and surface characteristics of catalysts are of paramount importance in determining the efficiency and effectiveness of both carbon reduction and oxygen reduction processes. By elaborately tuning and optimizing the catalyst's structural and surface features, the reaction kinetics and selectivity can be significantly enhanced, leading to improved overall performance.[54,55] Furthermore, the minimization of precious metal content within the catalyst formulation can contribute to substantial reductions in material expenses. This strategic approach, which involves the strategic substitution or reduction of costly precious metal components, can help alleviate the financial burden associated with the deployment of these electrochemical systems into industrial-scale applications, thereby improving their economic viability and competitiveness.

Second, enabling customized ion delivery and reaction is also a major area of improvement for PSE equipment. Therefore, it is essential to select suitable solid electrolytes for corresponding reactions. The commonly used sulfonated copolymers are mainly used for proton transfer, while the PSE (Dowex 1 × 8 (formate-formed) (Sigma–Aldrich)) may hold the comparative ability for formate conduction and thus lower the energy loss in the middle chamber. Additionally, for the PSE reactor applied in an alkaline environment, a base-formed solid polymer electrolyte (Amberlite FPA66 (DuPont) or AmberChrom 1 × 8 (DuPont)) may hold considerable performance than a proton-formed one. Importantly, the modifications on membranes also serve vital functions for ion transport. The core of a PSE reactor lies in the deliberate and controlled migration of ions between the cathode and anode chambers. The utilization of ion exchange membranes should not be restricted solely to PEMs but should also encompass mono- and multi-valence cation exchange membranes. Sophisticated membranes endowed with high ionic

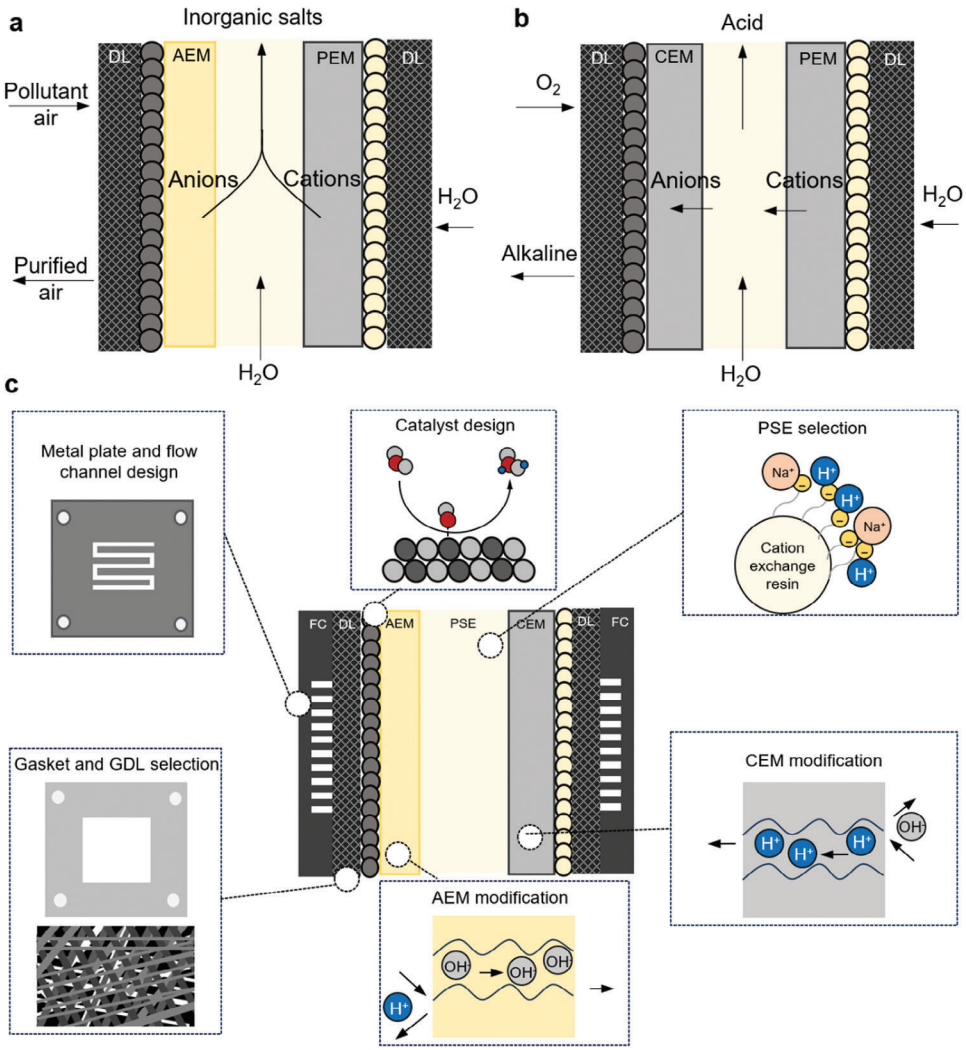

Figure 7. The possible applicationsd of the PSE reactors for a) air purification and b) heavy metal recovery. c) The schematic diagram of the components to be modified and optimized in the PSE reactor.

mobility, conductivity, and selectivity should be judiciously employed in PSE reactor systems. Regarding AEMs, the dual objectives of achieving high permeability and long-term durability can be attained through strategic modifications to the surface properties and porosity of these membranes. Furthermore, enhancing the membrane's tolerance to acidic environments remains an open challenge that warrants further investigation and study. The development of membranes with robust chemical stability and resilience to harsh operating conditions is crucial for the reliable and sustained operation of PSE reactors.

Third, the design and optimization of the solid-state electrolytes also has a significant impact on the electrosynthesis of pure products. A commonly used proton-conducting solid-state electrolyte is sulfonic acid functionalized, while other groups such as carboxylic acid groups[56,57] and phosphoric acid groups[58,59] that also have excellent proton conducting ability can also be assembled on dimeric solid-state electrolyte particles to achieve potentially even more proton conductivity. At the same time, due to the structure of the dimer backbone, the number of functionalized groups is limited, which means limited proton conduction. Therefore, the structural optimization of the solid-state electrolyte backbone is also an effective means and a feasible direction to improve the proton conduction ability of PSE. In addition, due to the compacting effect of the sandwich-type structure, the mechanical strength of the solid electrolyte particles and the tolerance to local strong acidic and alkaline environments are also aspects that need to be improved, which can be achieved by polymer cross-linking, modification and doping with inorganic fillers.

The gas diffusion layer (GDL) situated between the CL and the metal plate plays a crucial role in the uniform distribution of reactants and products. Consequently, the concentration-induced energy losses and contact resistance can be effectively mitigated by the utilization of porous, uniform, and stable diffusion support structures.[60,61] In the practical electrode preparation process, the GDL, serving as a substrate, is intimately bonded to the CL. As such, the GDL's hydrophobicity and electrical conductivity also exert a considerable influence on the electrocatalytic

reactions taking place. Additionally, the thickness of the gasket has a direct bearing on the contact resistance within the system. An excessively thick gasket can create an undesirably large gap between the GDL and the metal plate, thereby hindering the smooth and stable progression of the reaction. Conversely, an overly thin gasket can lead to an uneven distribution of compressive strength on the GDL, potentially damaging the support substrate and disrupting the reaction.

The terminal component is the metal plate, which encompasses the flow channels and the conduction plate. The appropriate design of the flow channels is of paramount importance, as it ensures the uniform distribution of reactants and the effective removal of products, while also facilitating the crucial thermal management of the reactor.[62,63] Consequently, the flow channel design is a central focus in the optimization and deployment of PSE reactors and merits in-depth and comprehensive investigation.[64] Meanwhile, the material selection for the metal plate is also a critical consideration, as it directly impacts the long-term durability and reliability of the PSE reactor system. Specific emphasis should be placed on the metal plate's resistance and tolerance to electrochemical corrosion and acidic environments. The judicious selection of corrosion-resistant materials is essential for maintaining the structural integrity and electrochemical performance of the PSE reactor over its lifetime of operation. In addition to flow channels on metal plates, the design of the flow channels in the central chamber warrants further attention. Given that the central chamber is involved in the ion recombination or separation of target products and filled with solid-state electrolyte particles, the appropriate concentration, pressure, and temperature distributions significantly influence the generation of products within this chamber. However, current research has not adequately addressed the flow channel design and fluid dynamics simulations related to the middle chamber. Future efforts in the design and optimization of PSE reactors should also prioritize these aspects. By focusing on the hydrodynamic behavior and ensuring optimal conditions within the central cavity, it can be predicted to obtain enhanced efficiency and effectiveness of ion transfer processes, ultimately improving product yield and purity.

The promising applications of PSE devices make the design and optimization for future industrialization particularly critical. In addition to the aforementioned optimization strategies, scalable designs for reactor components are essential for enabling PSE devices to operate at industrial-level currents.[65] While scaling the areas of the CL, GDL, and a membrane is relatively straightforward, the mass transfer effects related to the reactant delivery and product removal facilitated by the flow channels in the metal plates become increasingly important. Traditional single serpentine flow channel designs are inadequate to meet the mass transfer requirements at high current densities, necessitating the design of multiple parallel flow channels to minimize pressure differentials resulting from increased flow rates.[66,67] Moreover, thermal management of the device under industrial-level current densities is a significant factor affecting performance. Natural heat dissipation through the metal plate material alone is insufficient for the effective removal of heat from the reactor. One solution is to incorporate coolant flow channels throughout the reactor to transport excess heat away via water flow. Another approach involves creating an array of perforated grooves on the metal plates to enhance the contact area with air for natural convective heat transfer, thereby improving heat removal. Additionally, the current design of the intermediate cavity lacks flow channels for natural diffusion, and as the reaction area increases, the design of flow channels in the intermediate cavity will play a crucial role in the synthesis of target products. Therefore, the industrial application of PSE devices requires efforts not only in the design of electrocatalytic materials but also in the optimization of reactor flow channel designs and thermal management strategies.

6. Summary

In conclusion, the detailed reactor structure, components, and configurations, along with their corresponding applications, are comprehensively summarized. Future directions for the expansion of PSE reactors have been proposed, including air separation and purification, and heavy metal ion recovery. The revolutionary proposal of the PSE reactor enables a long-lasting and profound impact on the development of electrolytic cells. Driven by renewable energy, the reactor not only combines the advantages and improvements of conventional electrolyzers or fuel cells but also handles the issues of energy-intensive and process-complicated separation and purification by introducing a middle PSE chamber. Moreover, the modular, portable, and scalable features allow the PSE reactor to be employed in a series of different scenarios, ranging from micro-biodevices, indoor cleaning tools, and equipment for the synthesis of high-value-added products. In the future, the catalyst design should be combined with solid-state electrolyte modification, synthesis and selection, GDL and gasket regulation, flow channel design in metal plates and the middle plate, and anti-corrosion design of polar plates to promote the PSE reactors to an industrially scalable stage.

Acknowledgements

X.Z. acknowledges the support from Hong Kong Polytechnic University (CD9B, WZ4Q, CDBZ), the National Natural Science Foundation of China (22205187), Shenzhen Municipal Science and Technology Innovation Commission (JCYJ20230807140402006), and Department of Science and Technology of Guangdong Province (2023A1515110123, 2024A1515012390).

Conflict of Interest

The authors declare no conflict of interest.

Keywords

electrochemical CO2 capture, electrochemical liquid fuel production, electrochemical synthesis, solid-state electrolyte reactors

Received: August 26, 2024
Revised: September 30, 2024
Published online: October 20, 2024

[1] J. Zhang, L. Zhang, H. Liu, A. Sun, R.-S. Liu, in *Electrochemical Technologies for Energy Storage and Conversion*, Vol. *1*, John Wiley & Sons, New York **2011**.

[2] K. Scott, in *Sustainable and Green Electrochemical Science and Technology*, John Wiley & Sons, New York **2017**.
[3] M. J. Orella, Y. Román-Leshkov, F. R. Brushett, *Curr. Opin. Chem. Eng.* **2018**, *20*, 159.
[4] F. Cheng, J. Shen, B. Peng, Y. Pan, Z. Tao, J. Chen, *Nat. Chem.* **2011**, *3*, 79.
[5] L. F. Novaes, J. Liu, Y. Shen, L. Lu, J. M. Meinhardt, S. Lin, *Chem. Soc. Rev.* **2021**, *50*, 7941.
[6] D. A. Salvatore, D. M. Weekes, J. He, K. E. Dettelbach, Y. C. Li, T. E. Mallouk, C. P. Berlinguette, *ACS Energy Lett.* **2017**, *3*, 149.
[7] J. B. Greenblatt, D. J. Miller, J. W. Ager, F. A. Houle, I. D. Sharp, *Joule* **2018**, *2*, 381.
[8] D. M. Weekes, D. A. Salvatore, A. Reyes, A. Huang, C. P. Berlinguette, *Acc. Chem. Res.* **2018**, *51*, 910.
[9] T. Alerte, J. P. Edwards, C. M. Gabardo, C. P. O'Brien, A. Gaona, J. Wicks, A. Obradovic´, A. Sarkar, S. A. Jaffer, H. L. MacLean, *ACS Energy Lett.* **2021**, *6*, 4405.
[10] A. Sarswat, D. S. Sholl, R. P. Lively, *Sustainable Energy Fuels* **2022**, *6*, 4598.
[11] K. Xie, A. Ozden, R. K. Miao, Y. Li, D. Sinton, E. H. Sargent, *Nat. Commun.* **2022**, *13*, 3070.
[12] C. Xia, Y. Xia, P. Zhu, L. Fan, H. Wang, *Science* **2019**, *366*, 226.
[13] C. Xia, P. Zhu, Q. Jiang, Y. Pan, W. Liang, E. Stavitski, H. N. Alshareef, H. Wang, *Nat. Energy* **2019**, *4*, 776.
[14] P. Zhu, C. Xia, C.-Y. Liu, K. Jiang, G. Gao, X. Zhang, Y. Xia, Y. Lei, H. N. Alshareef, T. P. Senftle, *Proc. Natl Acad. Sci. USA* **2021**, *118*, e2010868118.
[15] P. Zhu, H. Wang, *Nat. Catal.* **2021**, *4*, 943.
[16] Y. Wen, T. Zhang, J. Wang, Z. Pan, T. Wang, H. Yamashita, X. Qian, Y. Zhao, *Angew. Chem.* **2022**, *134*, e202205972.
[17] Y. Kang, T. Kim, K. Y. Jung, K. T. Park, *Catalysts* **2023**, *13*, 955.
[18] Z. B. Zhang, B. Fang, G. Liu, *Device* **2023**, *1*, 3.
[19] S. Günday, A. Bozkurt, W. H. Meyer, G. Wegner, *J. Polym. Sci. B* **2006**, *44*, 3315.
[20] S. Martwiset, O. Yavuzcetin, M. Thorn, C. Versek, M. Tuominen, E. B. Coughlin, *J. Polym. Sci., Part A: Polym. Chem.* **2009**, *47*, 188.
[21] W. A. England, M. Cross, A. Hamnett, P. Wiseman, J. B. Goodenough, *Solid State Ion.* **1980**, *1*, 231.
[22] J. Millar, D. Smith, W. Marr, T. Kressman, *J. Chem. Soc. (Resumed)* **1963**, 218.
[23] R. L. Albright, *React. Polym., Ion Exch., Sorbents* **1986**, *4*, 155.
[24] L. Yue, J. Ma, J. Zhang, J. Zhao, S. Dong, Z. Liu, G. Cui, L. Chen, *Energy Storage Mater.* **2016**, *5*, 139.
[25] S. Lüftl, E. Richaud, in *Polyoxymethylene Handbook: Structure, Properties, Applications and Their Nanocomposites*, Wiley, New York **2014**, pp. 277–299.
[26] P. Zhu, Z.-Y. Wu, A. Elgazzar, C. Dong, T.-U. Wi, F.-Y. Chen, Y. Xia, Y. Feng, M. Shakouri, J. Y. Kim, *Nature* **2023**, *618*, 959.
[27] H. D. Willauer, F. DiMascio, D. R. Hardy, M. K. Lewis, F. W. Williams, *Ind. Eng. Chem. Res.* **2011**, *50*, 9876.
[28] H. D. Willauer, F. DiMascio, D. R. Hardy, F. W. Williams, *Energy Fuels* **2017**, *31*, 1723.
[29] E. Komkova, D. Stamatialis, H. Strathmann, M. Wessling, *J. Membr. Sci.* **2004**, *244*, 25.
[30] Z. Yang, J. Ran, B. Wu, L. Wu, T. Xu, *Curr. Opin. Chem. Eng.* **2016**, *12*, 22.
[31] C. G. Arges, L. Zhang, *ACS Appl. Energy Mater.* **2018**, *1*, 2991.
[32] R. O'Hayre, D. M. Barnett, F. B. Prinz, *J. Electrochem. Soc.* **2005**, *152*, A439.
[33] L. Fan, C. Xia, P. Zhu, Y. Lu, H. Wang, *Nat. Commun.* **2020**, *11*, 3633.
[34] J. Zhu, J. Li, R. Lu, R. Yu, S. Zhao, C. Li, L. Lv, L. Xia, X. Chen, W. Cai, *Nat. Commun.* **2023**, *14*, 4670.
[35] T. Zheng, C. Liu, C. Guo, M. Zhang, X. Li, Q. Jiang, W. Xue, H. Li, A. Li, C.-W. Pao, *Nat. Nanotechnol.* **2021**, *16*, 1386.
[36] H. Yang, J. J. Kaczur, S. D. Sajjad, R. I. Masel, *J. CO2 Util.* **2017**, *20*, 208.
[37] H. Yang, J. J. Kaczur, S. D. Sajjad, R. I. Masel, *J. CO2 Util.* **2020**, *42*, 101349.
[38] H. Yang, N. Han, J. Deng, J. Wu, Y. Wang, Y. Hu, P. Ding, Y. Li, Y. Li, J. Lu, *Adv. Energy Mater.* **2018**, *8*, 1801536.
[39] B. Q. Miao, W. S. Fang, B. Sun, F. M. Li, X.-C. Wang, B. Y. Xia, Y. Chen, *Chin. J. Struct. Chem.* **2023**, *42*, 100095.
[40] N. Han, Y. Wang, H. Yang, J. Deng, J. Wu, Y. Li, Y. Li, *Nat. Commun.* **2018**, *9*, 1320.
[41] X. Wang, Z. Wang, T.-T. Zhuang, C.-T. Dinh, J. Li, D.-H. Nam, F. Li, C.-W. Huang, C.-S. Tan, Z. Chen, *Nat. Commun.* **2019**, *10*, 5186.
[42] T. Zheng, M. Zhang, L. Wu, S. Guo, X. Liu, J. Zhao, W. Xue, J. Li, C. Liu, X. Li, *Nat. Catal.* **2022**, *5*, 388.
[43] X. Yan, M. Zhang, Y. Chen, Y. Wu, R. Wu, Q. Wan, C. Liu, T. Zheng, R. Feng, J. Zhang, *Angew. Chem.* **2023**, *135*, e202301507.
[44] Y. Xia, X. Zhao, C. Xia, Z.-Y. Wu, P. Zhu, J. Y. Kim, X. Bai, G. Gao, Y. Hu, J. Zhong, *Nat. Commun.* **2021**, *12*, 4225.
[45] X. Zhang, X. Zhao, P. Zhu, Z. Adler, Z.-Y. Wu, Y. Liu, H. Wang, *Nat. Commun.* **2022**, *13*, 2880.
[46] B. S. Rawah, M. Albloushi, W. Li, *Chem. Eng. J.* **2023**, *466*, 143282.
[47] D. Reinisch, B. Schmid, N. Martić, R. Krause, H. Landes, M. Hanebuth, K. J. Mayrhofer, G. Schmid, *Z. Phys. Chem.* **2020**, *234*, 1115.
[48] G. O. Larrazábal, P. Strøm-Hansen, J. P. Heli, K. Zeiter, K. T. Therkildsen, I. Chorkendorff, B. Seger, *ACS Appl. Mater. Interfaces* **2019**, *11*, 41281.
[49] J. Y. T. Kim, P. Zhu, F.-Y. Chen, Z.-Y. Wu, D. A. Cullen, H. Wang, *Nat. Catal.* **2022**, *5*, 288.
[50] L. Fan, Y. Zhao, L. Chen, J. Chen, J. Chen, H. Yang, Y. Xiao, T. Zhang, J. Chen, L. Wang, *Nat. Catal.* **2023**, *6*, 585.
[51] S. K. Zhang, Y. Feng, A. Elgazzar, Y. Xia, C. Qiu, Z. Adler, C. Sellers, H. Wang, *Joule* **2023**, *7*, 1887.
[52] G. Kolyagin, V. Kornienko, *Russ. J. Appl. Chem.* **2006**, *79*, 746.
[53] F. Y. Chen, A. Elgazzar, S. Pecaut, C. Qiu, Y. Feng, S. Ashokkumar, Z. Yu, C. Sellers, S. Hao, P. Zhu, *Nat. Catal.* **2024**, *7*, 1032.
[54] P. D. Liu, A. G. Liu, P. M. Wang, Y. Chen, B. Li, *Chin. J. Struct. Chem.* **2023**, *42*, 100001.
[55] K. Wang, J. Wu, S. Zheng, S. Yin, *Chin. J. Struct. Chem.* **2023**, *42*, 100104.
[56] A. Bozkurt, W. H. Meyer, G. Wegner, *J. Power Sources* **2003**, *123*, 126.
[57] A. Shigematsu, T. Yamada, H. Kitagawa, *J. Am. Chem. Soc.* **2011**, *133*, 2034.
[58] R. He, Q. Li, G. Xiao, N. J. Bjerrum, *J. Membr. Sci.* **2003**, *226*, 169.
[59] S. Ü. Çelik, A. Aslan, A. Bozkurt, *Solid State Ion* **2008**, *179*, 683.
[60] I. Nitta, O. Himanen, M. Mikkola, *Electrochem. Commun.* **2008**, *10*, 47.
[61] D. Ye, E. Gauthier, J. B. Benziger, M. Pan, *J. Power Sources* **2014**, *256*, 449.
[62] R. Boddu, U. K. Marupakula, B. Summers, P. Majumdar, *J. Power Sources* **2009**, *189*, 1083.
[63] T. Wilberforce, Z. El Hassan, E. Ogungbemi, O. Ijaodola, F. Khatib, A. Durrant, J. Thompson, A. Baroutaji, A. Olabi, *Renew. Sustainable Energy Rev.* **2019**, *111*, 236.
[64] J.-K. Kuo, T.-S. Yen, *Energy Convers. Manage.* **2008**, *49*, 2776.
[65] K. Ayers, *Curr. Opin. Chem. Eng.* **2021**, *33*, 100719.
[66] S. M. Baek, D. H. Jeon, J. H. Nam, C.-J. Kim, *J. Mech. Sci. Technol.* **2012**, *26*, 2995.
[67] L. Rostami, M. Haghshenasfard, M. Sadeghi, M. Zhiani, *Energy* **2022**, *258*, 124726.

Weisong Li is currently a Ph.D. student from Dr. Xiao Zhang's group at the Department of Mechanical Engineering at Hong Kong Polytechnic University. He received his B.Sc. and M.Sc. in chemical engineering and technology, and advanced chemical engineering from Xi'an Polytechnic University (China) and The University of Manchester (UK) in 2017 and 2019, respectively. He then worked in chemical unit operation, on-site pilot testing, and engineering control from 2020 to 2022. Currently, he mainly concentrates on electrochemical carbon capture, electrochemical gas pollutant removal, and electrochemical reactor optimization and design.

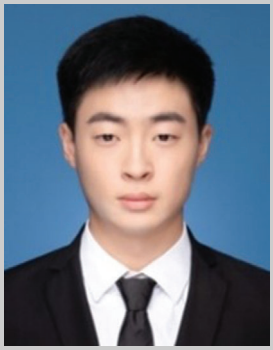

Yanjie Zhai is a Ph.D. candidate under the supervision of Dr. Xiao Zhang at the Department of Mechanical Engineering at Hong Kong Polytechnic University. He received his B.Sc. and M.Sc. in materials science and engineering from Shandong University (China) in 2016 and 2019, respectively. He then joined Fudan University (China) and Shandong Academy of Sciences as a research assistant before studying at The Hong Kong Polytechnic University in 2021. Currently, he mainly focuses on the electrochemical production of high-valuable chemicals/fuels from small molecules and the electrochemical reactor design toward specific catalytic reactions.

Qing Xia is a Ph.D. candidate in the Department of Mechanical Engineering at The Hong Kong Polytechnic University. He received his M.S. from Shandong University. His dissertation focuses on catalyst design and electrochemical reactor design for the conversion of small molecules.

Xiao Zhang is currently an Assistant Professor in the Department of Mechanical Engineering at The Hong Kong Polytechnic University. He received his PhD degree from Nanyang Technological University (Singapore) in 2017 and continued his research in the same group as a Research Fellow for two years. Prior to joining the Hong Kong Polytechnic University, he was a Rice Academy Junior Fellow at Rice University (US). His current research interests focus on the electrochemical production of high-valuable chemicals/fuels from atmospheric molecules (O_2, H_2O, CO_2, NO_3^-), the design of an appropriate electrocatalytic interface, and the electrochemical reactor toward specific catalytic reactions.